IET Journals
The Institution of Engineering and Technology

Effects of Plastic Vehicular Covers on Radiation Characteristics of Lightweight, Dual-band Antenna for Vehicular Communications

ISSN 1751-8644
doi: 0000000000
www.ietdl.org

Adamantia Chletsou[1], *John F. Locke*[2], *John Papapolymerou*[3]

[1] *Electrical and Computer Engineering, Michigan State University, East Lansing, Michigan, USA*
[2] *Ford Motor Company, Dearborn, Michigan, USA*
[3] *Electrical and Computer Engineering, Michigan State University, East Lansing, Michigan, USA*
* *E-mail: chletsou@egr.msu.edu*

Abstract: This paper highlights the impact of curved and flat vehicular plastic parts on the radiation characteristics of two dual-band antennas for C-V2X applications. The radiation patterns of the antennas are measured in SATIMO near field measurement system and are compared during the following setups: (a) antennas alone in the near field system, without the presence of a plastic part; (b) antennas mounted on the inside curved surface of a driver's side mirror cover; (c) antennas mounted on the outside curved surface of the driver's side mirror cover; (d) antennas mounted on a flat trunk lid; (e) antennas mounted on a curved plastic retrieved from the A-pillar of a vehicle. Comparison among the antennas radiation pattern measurements during these five different setups, results in the conclusion that the inside surface of the side mirror cover is the most suitable position to mount the presented dual-band antennas. The curvature of the inside surface at the point where the antenna was mounted is less steep than the placement point at the outside surface, allowing the antenna to keep its polarization axis mostly unaffected. Moreover, the curve of the inside surface makes the antenna radiation more directional, creating an increase in the antenna gain. The side mirror cover, compared to trunk lid, is further from the ground protecting the antenna radiation from additional reflections.

1 Introduction

The cellular and Cellular Vehicle To Everything (C-V2X) bands have gained great attention the last few years for enabling vehicles to communicate with their surroundings at higher rates. Some potential applications of the C-V2X technology includes communication between a vehicle and the network (V2N), a vehicle and the infrastructure (V2I), a vehicle and a pedestrian (V2P) and two vehicles (V2V). The C-V2X is a novel technology and as such its infrastructure is under development. For this reason, the suggested antenna is desired to cover frequencies within the cellular bands and take advantage of the already deployed cellular network infrastructure.

The evolving technology of vehicular communications demands the use of numerous antennas but the metal nature of the vehicle body restricts the places where an antenna can operate normally. As a result multi-band antennas and antennas on a flexible substrate that can be adjusted on vehicle plastic parts, occupying limited space, are at high demand. Most of the cellular antennas are implemented on a rigid substrate and are placed inside a shark fin on a rooftop of a vehicle, using the metal rooftop as a ground plane. Recently though, other parts of the vehicle are being investigated to house an antenna. In [1] the authors tested an antenna created on a thin flexible $35\mu m$ copper foil with adhesive for WLAN applications and placed it into the plastic spoiler of a hatchback. In [2] the use of diversity antennas for Vehicle to Vehicle (V2V) applications was researched by placing antennas on the rooftop, side mirror, windscreen and bumper. The authors at [3] investigated numerically the effects of the car body on the radiation of an antenna used for inter-vehicle communications, when it is placed on a side mirror. Circularly polarized antennas covering the 2.5-2.57 GHz, 2.62-2.69 GHz and 3.4-3.8 GHz bands were implemented and measured on a planar and curved surface, imitating the side mirror cover in [4]. The antennas are created on the flexible polyimide substrate. Another antenna operating at 5.9 GHz for Truck-to-Truck communications is developed in [5]. The Electronically Switched Parasitic Array Radiator (ESPAR) antenna is implemented on the rigid RO4725-JXR substrate and tested behind a mirror cover in the lab. In [6] the authors investigate the effect of the antenna position on its radiation. An antenna operating at 700 MHz, 2600MHz and 5870 MHz was mounted on different positions on a vehicle's rooftop. Measurements on the various locations showed that the effect of the mounting location is negligible at lower frequencies, but as the frequency tends to increase, it becomes significant. The authors in [7] address the influence of the plastic embedding and the door frame on the performance of the antenna. The ABS on the door frame affects the antenna frequency of operation by causing a shift to it. This is observed in this paper, too, when the antenna is mounted on the mirror cover, the trunk lid, and the A-pillar.

This letter contributes to the knowledge of the impact of the different shaped automotive plastic parts on the radiation of the antenna at the cellular and Cellular-Vehicle To Everything (C-V2X) bands. Compared to the literature, this research investigates the effect of the different shapes of automotive plastic surfaces on cellular and C-V2X antenna radiation performance. In [8] a similar antenna design is tested outdoors, on a real convertible car, to investigate the effects of the entire vehicle platform and ground on the antenna performance. In contrast to the study presented in this paper, the different shapes and surfaces of the automotive parts were not taken into consideration in [8]. Moreover, the antenna performance in [8] was studied in a far field setup taking into account the disturbances caused by the outside environment. In this research the antenna performance is measured in a near field system, with absorbing structures around the Antenna Under Test (AUT), limiting the measurements to examine only the effect of the shape and the surface of the automotive part on the antenna radiation pattern.

To the best of our knowledge this is the first research about optimal antenna placement on different in shape automotive plastics and it can be used for deciding embedded antenna locations in future vehicles.

Two different antenna designs, implemented on the flexible Rogers 3850 (Liquid Crystalline Polymer) substrate are mounted on

a plastic trunk lid, a mirror cover and a curved plastic retrieved from the inside of a real vehicle. The radiation patterns, efficiency and realized gain of the antennas mounted on the automotive parts are measured in Satimo SG32 near field system. The performance of the antennas presented in this paper on the various plastic parts is compared to the performance of the antennas in literature in Table 1. The maximum realized gain values reported on 1 of this work refer to the measurements of the antennas alone, without any plastic below them and when they are mounted on the inside surface of the side mirror cover. The term free under the column of antenna position in vehicle in table 1 refers to the antenna measurements when they are measured alone, when there is no plastic below them. The term curved in the same column of the table refers to the placement of the antenna on the inside surface of the side mirror. Compared to the antennas in literature, the antennas presented here operate at two frequencies with a wavelength ratio of 7. At 800 MHz the antennas have omni-directional radiation pattern whereas the antennas in [1] have directional radiation pattern. When comparing the antenna measurements in free space, where the antennas lie flat, and on the curved surface, the values of the maximum realized gain slightly increase for antenna 1, as in [4]. At 5.9 GHz both antennas presented here have a slightly lower maximum value of realized gain compared to the [5]. Namely the authors of [5] state a maximum value of gain around 5 dBi but the antenna 1 and 2 measured here have a gain of 4.6 and 4.2 dBi when measured alone in the Satimo near field system. When placing the antenna 2 on the trunk lid which is a flat plastic, similar to the door frame of [7] the maximum realized gain at 800 MHz is 0.43 dBi and at 5.9 GHz around 5.5 dBi. The gain of the antenna in [7] on the flat plastic is around 3.5 dBi at 2.45 GHz.

In Section I, the design of the antennas and their simulation results in Ansys EM software are presented. Then the S_{11} parameters as measured with the M5227 Keysight Personal Network Analyzer and the radiation patterns of the antennas without any plastic below them, as measured in the Satimo SG32 near field system are studied. The radiation patterns of the antennas when mounted on the automotive plastic parts as retrieved by the Satimo near field system are presented. Finally, the radiation patterns of the antennas from each placement are analyzed and the best position on the plastic part for antenna mounting is selected.

2 Antenna design

The antennas tested in this paper have similar design. They both consist of a bow-tie which extends to meander lines and are fed by a strip-line with an SMA connector. The logic behind this design is that the antenna is dual band and resonates at the cellular 4G frequencies (below 1GHz) and at the high C-V2X, 5.9 GHz. The bow-tie is resonating at 5.9 GHz and the meander lines provide the resonance at the lower cellular frequencies. At the lower cellular frequency the antenna has a TM resonant mode, like an electric dipole but in the higher C-V2X frequency the antenna has a hybrid TE/TM mode due to the size of the meander lines and the feed-line. Both the antenna designs are indicated in Fig.1 and Fig.2 and their dimensions in Table 2. The antennas are implemented on the flexible Rogers 3850 (LCP) using lithography. The LCP has a permittivity of $\epsilon_r = 2.9$ at 10GHz, $tan\delta = 0.0025$ and thickness $t = 0.1$mm, as stated in [9].

Table 1 Comparison of this work to the literature

Reference	Antenna Dimensions (mm^3)	Resonance frequencies (GHz)	Antenna position on vehicle	Maximum Realized Gain (dBi)
[1]	$2 * \lambda$	2.45	spoiler	12
[4]	44*42*0.1	3.575	planar	3.77
		3.45	curved	3.87
[5]	26*18*0.815	5.9	flat side mirror	5
[7]	73.9*36.9*1.6	2.45	door frame	3.5
This work	120*70*0.1	0.8	free	1.68
Antenna1		5.9	free	4.6
		0.85	curved	2.5
		5.9	curved	4.8
This work	100*70*0.1	0.8	free	1.6
Antenna2		5.9	free	4.2
		0.8	curved	0.187
		5.9	curved	1.54

3 Methods - Antenna simulations and measurements in Satimo near field system

The antennas are initially simulated in Ansys EM (HFSS) software. They are designed on the LCP substrate with an SMA connector at the edge of the slotline. The antenna design A is presented in detail in [10]. At cellular bands this antenna resonates at 817.6 MHz and has an efficiency of 89.8%. The maximum realized gain, according to the

Table 2 Antenna dimensions

Antenna Design	Variable	Dimensions (mm)
Design 1	a1	120
	b1	70
	c1	77.4
	d1	22.8
	e1	16.6
	f1	30.8
	g1	9.8
	h1	10.1
	j1	26
	k1	6.5
Design 2	a2	100
	b2	70
	c2	75.5
	d2	30.5
	e2	20
	f2	13.5
	g2	10
	h2	16.5
	j2	33

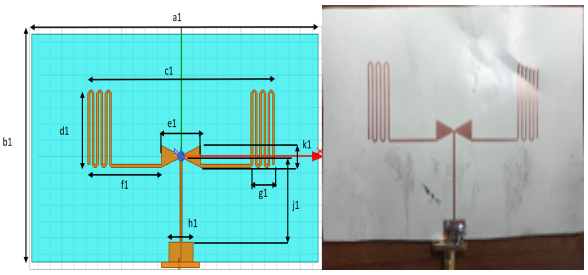

(a) (b)

Fig. 1: (a)Simulated and (b)implemented antenna A
a Simulation of antenna A
b Implemented antenna A

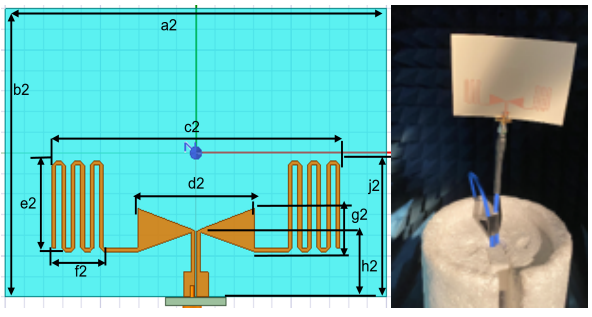

(a) (b)

Fig. 2: (a)Simulated and (b)implemented antenna B
a Simulation of antenna B
b Implemented antenna B

simulations is 0.99 dBi. At 5.9 GHz according to Ansys EM, the S_{11} is around -10 dB and the maximum realized gain around 2.79 dBi. The efficiency is 98.8%. The antenna A has an efficiency of 99.7% at C-V2X frequency. The S_{11} at 817.6 MHz is around -9 dB and at 5.9 GHz is around -10 dB. The antenna design B resonates at 886 MHz and at 5.9 GHz has an S_{11} of -17 dB. At cellular frequencies it has an efficiency of 94.6% and a maximum realized gain of 0.8 dBi. At C-V2X frequencies the simulations give a 100% efficiency and a maximum realized gain of 2.96 dBi.

The antennas are implemented using lithography and an SMA connector is soldered at their feed-line. A balUn is not used as simulations showed that omitting a balUn does not have an impact on the antenna performance at the frequencies of interest. The S-parameters of the manufactured antennas are measured using the M5227 PNA by Keysight Technologies. Then the antennas radiation performance and total efficiency are measured in the Satimo near field system under seven different measurement setups: (a) the antenna A alone, without any automotive plastic part below it; (b) the antenna A mounted inside the mirror cover of a vehicle, after having removed the metallic parts that were inside the mirror; (c) the antenna A mounted on the outer surface of the same mirror cover; (d) the antenna B alone, without the presence of any automotive plastic part; (e) the antenna B mounted outside of a mirror cover, after having removed the metallic parts from the inside of the cover; (f) the antenna B mounted on a flat trunk lid; (g) the antenna B placed on a curved plastic from the A-pillar of a vehicle.

3.1 Stand alone Antennas, no plastic below them

The implemented antenna A resonates at 771.7 MHz and at 5.9 GHz has an S_{11} of -15 dB, as shown in 3. Compared to the simulations, there is a resonance shift of only 46 MHz. The E-and H-plane of the antenna A at cellular and C-V2X frequencies without the presence of any automotive plastic, are indicated in Fig. 4, 5 and [10] with more details. At cellular frequency the measured efficiency of antenna A is 70.6% and the value of the maximum realized gain is 1.68 dBi. At 5.9 GHz, antenna A has an efficiency of 84.9% and the maximum value of the realized gain is 4.6 dBi. The efficiency measured inside the near field chamber represents the total efficiency of the antennas which includes the mismatch at each frequency. The total efficiency is the product of the radiation efficiency multiplied by the mismatch loss.

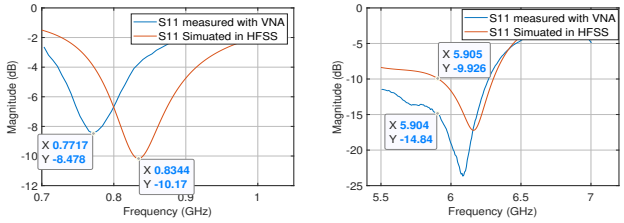

(a) (b)

Fig. 3: S_{11} parameters of simulated and implemented antenna A
a S_{11} parameters of simulated and implemented antenna A in cellular frequencies
b S_{11} parameters of simulated and implemented antenna A in C-V2X frequencies

The implemented antenna B resonates at 830 MHz and at 5.9 GHz has a measured S_{11} of -12.2 dB. When compared to the simulations there is a shift of 50 MHz to the resonance frequency at the cellular frequencies. This small shift in resonance frequency can be explained by fabrication tolerance. At 830 MHz it has an efficiency of 83% and the maximum realized gain as measured in Satimo system is 1.6 dB. At 5.9 GHz the efficiency of the antenna is measured at 81.2% and the maximum realized gain at 4.2 dBi. The S_{11} parameters of the implemented antenna are given in Fig. 6 for both frequency bands. The radiation patterns of the antenna without the presence of an automotive plastic, on E- and H-planes are given in Fig. 7 and Fig. 8 for cellular and C-V2X frequencies, respectively. At C-V2X there is a resonance shift of 394 MHz. This can be explained

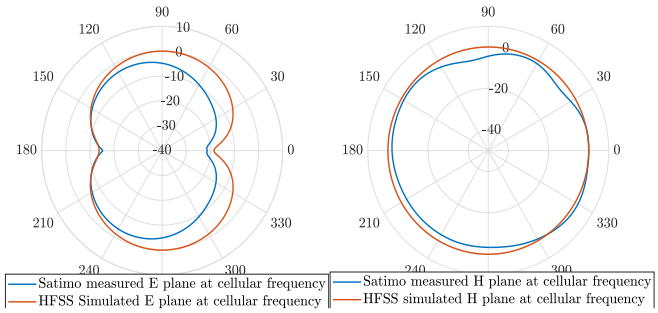

(a) (b)

Fig. 4: The simulated and measured radiation patterns of antenna A at cellular frequencies, without any automotive plastic
a E-plane
b H-plane

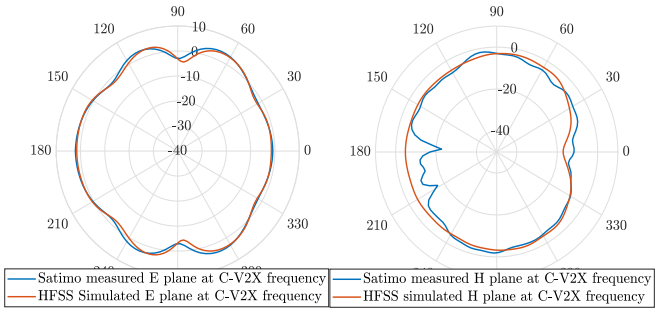

(a) (b)

Fig. 5: The simulated and measured radiation patterns of antenna A at C-V2X frequencies, without any automotive plastic
a E-plane
b H-plane

by the soldering size of the SMA connector. In simulations the soldering is represented by flat rectangles, extending the feeding pads and connecting them to the SMA, with a thickness of 1mil. In reality the soldering consists of two bulbs covering the whole feeding-pads and extending to the connector. At 5.9 GHz the wavelength is only 50mm which means that the thickness of the soldering can affect the resonance of the antenna.

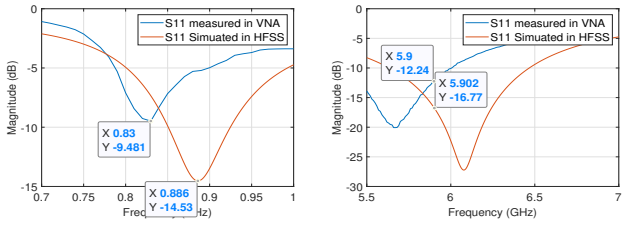

(a) (b)

Fig. 6: S_{11} parameters of simulated and implemented antenna B
a S_{11} parameters of simulated and implemented antenna B in cellular frequencies
b S_{11} parameters of simulated and implemented antenna B in C-V2X frequencies

3.2 Antennas tested with mirror cover

At a second step the antennas are mounted on a mirror cover that is empty from the inside and placed inside the Satimo near field system to measure their radiation patterns and efficiency. The mirror cover is made by Acrylonitrile Butadiene Styrene (ABS) which has a permittivity of $\epsilon_r = 2.5$ and $tan\delta = 0.004$ as measured by Agilent E4991A RF Impedance Material Analyzer in the lab. Antenna

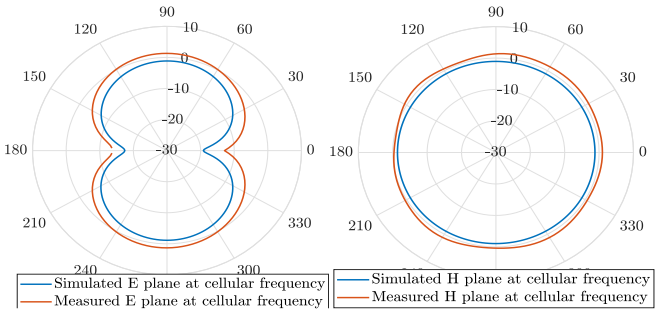

(a) (b)

Fig. 7: The simulated and measured radiation patterns of antenna B at cellular frequencies, without any automotive plastic
a E-plane
b H-plane

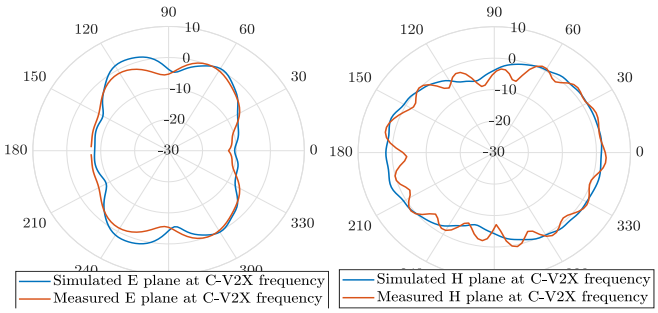

(a) (b)

Fig. 8: The simulated and measured radiation patterns of antenna B at C-V2X frequencies, without any automotive plastic
a E-plane
b H-plane

A is mounted initially inside the mirror cover. Electrical tape is used to stabilize the antenna and the coaxial cable inside the cover. Then the cover is placed back on the mirror skeleton as indicated on Fig. 9. The antenna realized gain and efficiency are measured at 800 MHz

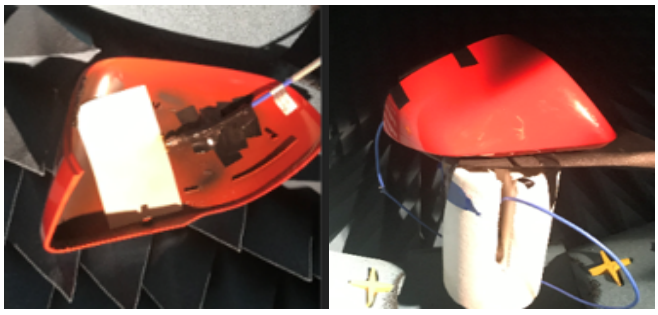

(a) (b)

Fig. 9: Antenna A inside the mirror
a mounted inside the mirror cover
b inside the side mirror

and 5.9 GHz. According to HFSS simulations, when a flat ABS part is placed below the Rogers 3850 substrate the resonance shifts from 816 MHz to 800 MHz and from 5.9 GHz to 5.3 GHz, for antenna A, as shown in Fig. 10. This is expected since adding a material with high permittivity below the antenna substrate, the effective wavelength decreases but the size of the antenna is the same so the antenna now will resonate to lower frequency. The antenna has a measured efficiency of 55.5% at 800 MHz and the maximum realized gain is 2.5 dBi for $\theta = 114^o$, as shown in Fig. 11. The realized gain is measured at 5.9 GHz since this is the frequency of interest for C-V2X applications. The antenna has a measured efficiency of 74.7% and a measured maximum realized gain of 4.8 dBi. The radiation patterns of the antenna A in this placement are given in Fig. 12.

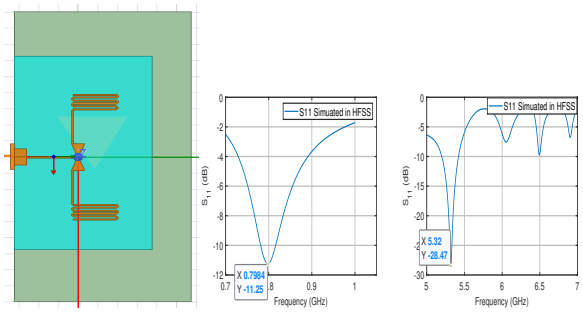

(a) (b) (c)

Fig. 10: Antenna A with ABS below the Rogers3850 substrate and the simulated S_{11} of antenna A with ABS below the Rogers 3850 substrate at cellular frequencies and at C-V2X frequency
a Antenna A with ABS below the Rogers3850 substrate
b Simulated S_{11} of antenna A with ABS below the Rogers 3850 substrate at cellular frequencies
c Simulated S_{11} of antenna A with ABS below the Rogers 3850 substrate at C-V2X frequency

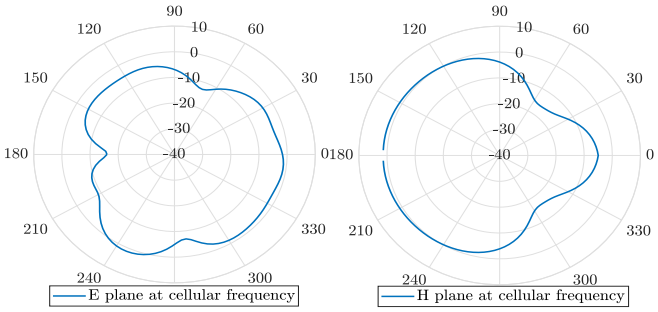

(a) (b)

Fig. 11: Radiation patterns of antenna A when mounted inside the mirror cover at 800 MHz
a E-plane
b H-plane

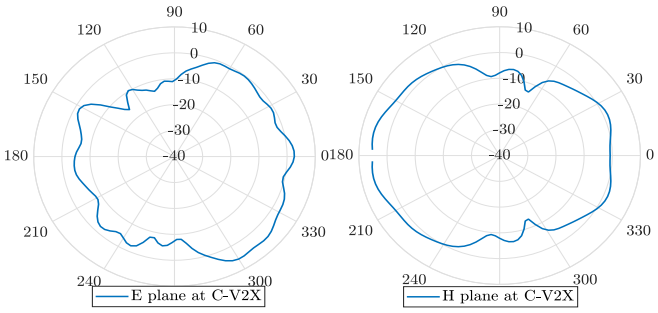

(a) (b)

Fig. 12: Radiation patterns of antenna A when mounted inside the mirror cover at 5.9 GHz
a E-plane
b H-plane

At a second step, the antenna A is mounted on the outer surface of the same mirror cover. The radiation patterns of the antenna A at this placement are demonstrated in Fig. 13 and 14 at the cellular and C-V2X frequencies respectively. The efficiency of the antenna A at cellular frequency when mounted on the outer surface of the mirror is 28% and has a maximum realized gain of -0.34 dBi. At C-V2X frequencies its measured efficiency is 63.4% and the maximum realized gain is 4dBi.

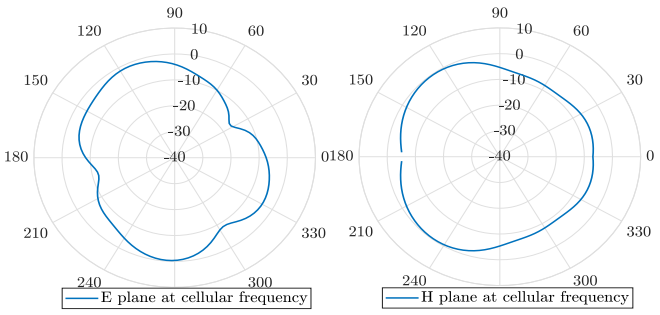

(a) (b)

Fig. 13: Radiation patterns of antenna A when mounted on the outside surface of the mirror cover at 800 MHz
a E-plane
b H-plane

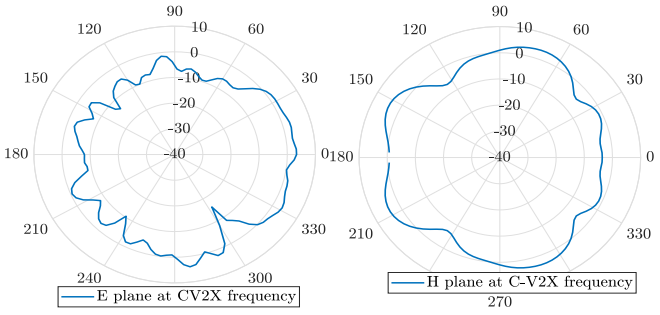

(a) (b)

Fig. 14: Radiation patterns of antenna A when mounted on the outside surface of the mirror cover at 5.9 GHz
a E-plane
b H-plane

The antenna B is also mounted on the outside surface of the side mirror cover, as indicated in Fig.16. Tape and a styrofoam are used to stabilize the antenna with the coaxial cable on the mirror cover in the Satimo system. The antenna B radiation pattern is measured at 800 MHz when it is mounted on ABS part because according to S_{11} measurements of antenna B on a piece of the trunk lid which is a flat ABS surface, below the Rogers 3850, the antenna B resonates at 800 MHz for the cellular frequencies, as indicated in Fig.15. In simulations the antenna resonance has shifted to 768 MHz. At 800 MHz the antenna has a measured efficiency of 43.87% when mounted on the curved ABS surface of the mirror cover and a maximum realized gain of 0.187 dBi at this placement. At C-V2X frequencies the antenna has a measured S_{11} of -9 dB when it is mounted on the flat ABS surface of the trunk lid. The efficiency of the antenna B at 5.9 GHz when is mounted on the curved surface of the mirror cover is 31% and the maximum realized gain 1.54 dBi. The radiation patterns of the antenna B mounted on the outer surface of the mirror cover are given in Fig. 17 and Fig. 18 at 800 MHz and 5.9 GHz, respectively.

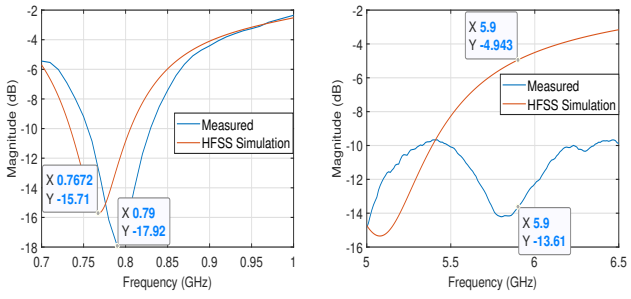

(a) (b)

Fig. 15: S_{11} parameters of antenna B when mounted on the trunk lid of a vehicle
a in cellular frequencies
b in C-V2X frequencies

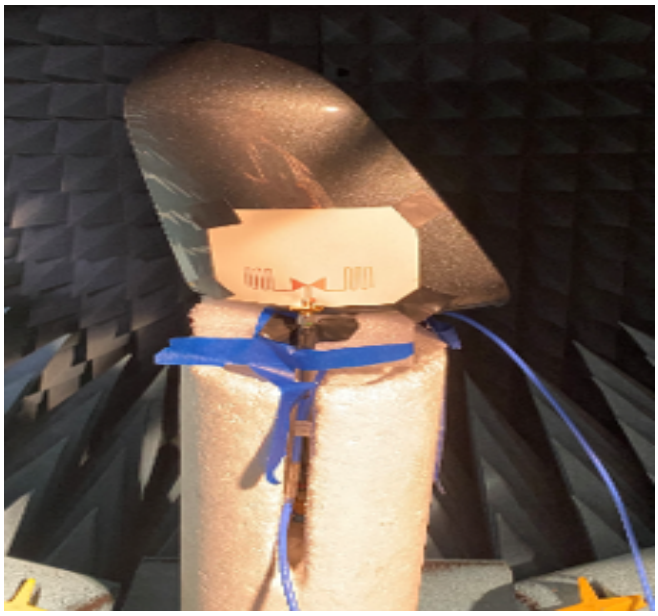

Fig. 16: Antenna B mounted on the outer surface of a mirror cover in the Satimo system

3.3 *Antenna B tested with the trunk lid*

The antenna B is mounted on a plastic trunk lid of a convertible vehicle using tape and transferred in Satimo system to measure its radiation patterns. In Ansys EM software the trunk lid is simulated as a flat ABS surface with thickness t=2.8 mm. The setup in Satimo is indicated in Fig.19. In Ansys EM software the antenna resonates around 768.4 MHz and has an S_{11} of -5 dB at 5.9 GHz. The implemented antenna when mounted on the real trunk lid resonates around 800 MHz and at 5.9 GHz has an S_{11} of -13.6 dB, as indicated in Fig.15. The efficiency of the simulated antenna B at 768.4 MHz is 93% and of the implemented is 51.4% at 800 MHz. At 5.9 GHz the simulated antenna has an efficiency of 89.5% when it is placed on the plastic ABS surface. In the near field system the efficiency is measured to be 71% at 5.9 GHz. The maximum realized gain of the antenna on the flat ABS according to Ansys EM software is 0.7 dBi at 768.4 MHz and 2.87 dBi at 5.9 GHz. The implemented antenna has a maximum realized gain of 0.4 dBi at 800 MHz and 2.5 dBi at 5.9 GHz when it is mounted on the trunk lid of the vehicle. The radiation patterns of the antenna B in this setup are given in Fig.20 and Fig.21. At cellular frequency the radiation patterns of the simulations match well with the radiation patterns of the measured antenna. The difference in the radiation patterns of the simulated to the manufactured antenna at C-V2X frequency can be explained by the size of the soldering. As explained before, the soldering of the SMA connector

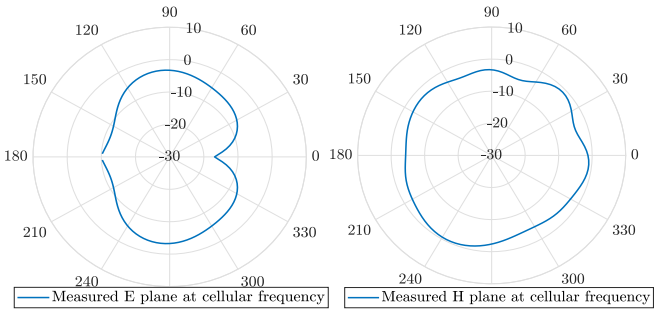

(a) (b)

Fig. 17: Radiation patterns of antenna B when mounted on the outer surface of the mirror cover at 800 MHz
a E-plane
b H-plane

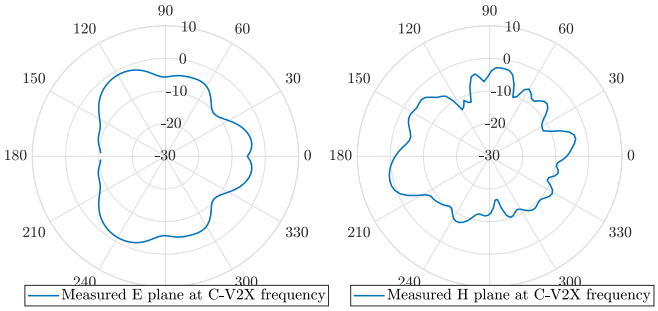

(a) (b)

Fig. 18: Radiation patterns of antenna B when mounted on the outer surface of the mirror cover at 5.9 GHz
a E-plane
b H-plane

on the implemented antenna consists of two big bulbs covering the whole feeding pads of the antenna. Whereas at the simulations, the soldering has a size of only 1mm $\times$ 0.25mm $\times$ 0.018mm.

Fig. 19: Antenna B mounted on the trunk lid of a real vehicle in the Satimo system

3.4 Antenna tested with the plastic retrieved from A-pillar of vehicle

The last experimental setup includes the antenna B mounted on a curved plastic retrieved from the A-pillar of a vehicle. The surface of this plastic is coarse and is not coated when compared to the ABS of the mirror cover and the trunk lid surfaces. The antenna B mounted on the A-pillar plastic and is indicated in Fig.22. The antenna has an efficiency of 36.75% at 800 MHz and a realized gain of 0.3 dBi at the same frequency. At 5.9 GHz the antenna has an efficiency of

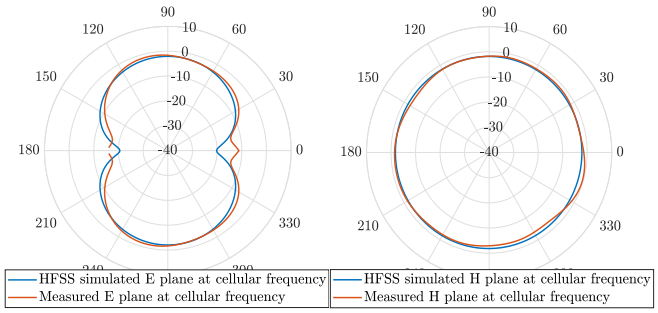

(a) (b)

Fig. 20: Radiation patterns of antenna B when mounted on the trunk lid of a vehicle at cellular frequencies
a E-plane
b H-plane

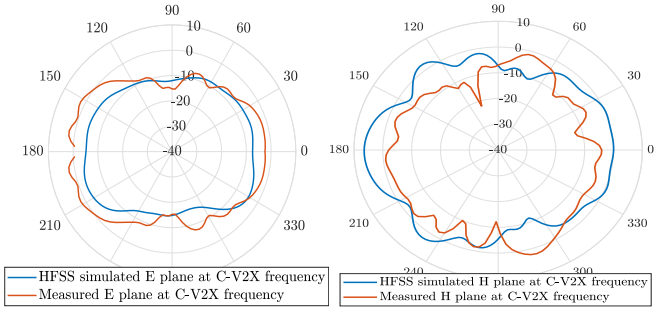

(a) (b)

Fig. 21: Radiation patterns of antenna B when mounted on the trunk lid of a vehicle at C-V2X frequencies
a E-plane
b H-plane

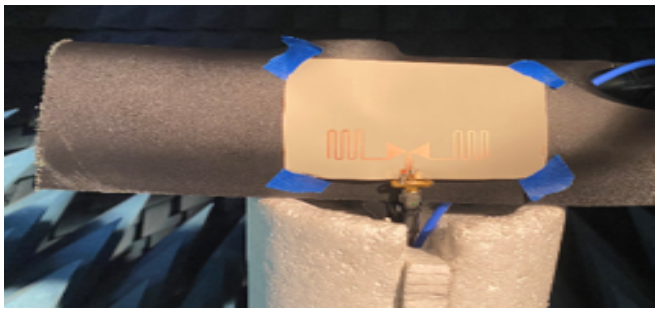

Fig. 22: Antenna B mounted on the A-pillar plastic of a real vehicle in the Satimo system

22% and a maximum realized gain of 1.9 dBi. The radiation patterns of the antenna on the curved plastic are shown in Fig.23 and 24.

4 Results and Discussion

The efficiency and maximum realized gain values of the various experimental setups are summarized in the table 3.

By comparing the results of the two antenna designs when they are measured alone, it is obvious that the values of the maximum realized gain are close for both the antennas. Their radiation patterns at cellular frequencies are similar. Both the antennas have an omni-directional radiation pattern at 800 MHz. At C-V2X their radiation patterns are different because antenna A has a longer slotline than antenna B and antenna B has longer meander lines. At 5.9 GHz the wavelength in free space is $\lambda = 50.8$mm and the size of the slotline as well as the meander lines is comparable to the wavelength. As

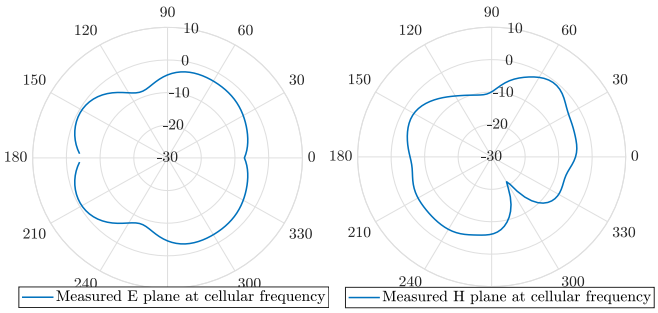

(a) (b)

Fig. 23: Radiation patterns of antenna B when mounted on a plastic from inside of the vehicle at cellular frequencies
a E-plane
b H-plane

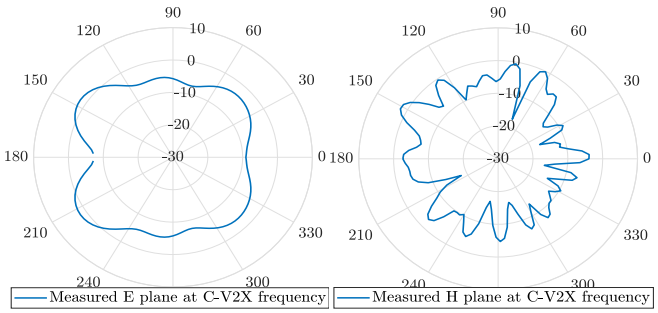

(a) (b)

Fig. 24: Radiation patterns of antenna B when mounted on a plastic from inside of the vehicle at C-V2X frequencies
a E-plane
b H-plane

a result there is radiation coming from the meander lines and the slotline at 5.9 GHz, which results to loss of the omni-directionality.

When placing the antennas on the ABS we expect that the resonance of the antennas will change. Namely, since the antenna size remains the same but the effective wavelength changes to $\lambda = \frac{c}{f\sqrt{\epsilon_r}}$, where ϵ_r refers to the electrical permittivity of ABS. The new effective wavelength is smaller but the antenna size remains the same, as a result the antenna resonates to lower frequencies when placed on ABS automotive parts, compared to when measured alone. This is also obvious in Fig.11a and Fig. 15a where the resonance of antenna B drops from 830 MHz to 800 MHz.

Table 3 Comparison of efficiency and maximum realized gain values at the different setups

Experimental Setup	Efficiency		Max Realized Gain (dBi)	
	Cellular	C-V2X	Cellular	C-V2X
Antenna A alone	50%	84.8%	1.64	4.6
Antenna B alone	82.9%	81.2%	1.6	4.2
Antenna A in mirror cover	40.3%	76%	1.38	4.6
Antenna A on mirror cover	26%	63.4%	-0.34	4
Antenna B on mirror cover	44%	31%	0.187	1.54
Antenna B on trunk lid	51.4%	71%	0.43	2.5
Antenna B on A-pillar	36.75%	22%	0.34	1.9

When mounting the antennas on the curved mirror cover there is a shift at the value of the maximum realized gains. Both antennas A and B have a decrease of the maximum realized gain value. The maximum realized gain of antenna A is 0.22 dBi higher at 800 MHz when the antenna is mounted on the inside surface of the mirror than when it is mounted on the outside surface of the same mirror cover. At 5.9 GHz the maximum realized gain is 0.6 dBi higher. When mounting the antenna A on the inner surface of the mirror cover, the radiation pattern on the H-plane becomes more directional compared to the radiation pattern of the same antenna when measured alone or on the outer surface of the same mirror cover at cellular frequency. When antenna A is mounted at the inner part of the mirror cover, it gets bent along the bowtie and meander direction, as a result the radiation patterns are modified. The radiated power gets concentrated in the concave direction as also proved in [11]. Kellomaki et al. study the effects of bending circular and linear polarized GPS antennas. According to their research the polarization of the tested patch antennas changed from circular to linear. Also the radiated power of the inverted-F antenna increased in the vertical and decreased in the horizontal polarization, compared to the unbent antenna. When the antenna A is mounted on the outer surface of the same mirror cover it gets bent on both directions, across and along the bowtie and meander lines. The radiation pattern on H-plane compared to the pattern of the same antenna when measured alone is more directional but compared to the pattern of the antenna mounted on the inner surface of the mirror cover, it is less directional. The efficiency of the antenna and the maximum realized gain values, at both cellular and C-V2X frequency bands, decrease.

When antenna B is mounted on the outer surface of the mirror cover, the maximum value of the realized gain drops almost 1.4 dBi at cellular frequencies, when compared to the measurements of the same antenna alone in the Satimo system and 2.66 dBi at C-V2X. The place where the antenna B is mounted on the mirror has a smaller bending radius than when mounting the antenna A on the inner surface of the mirror cover. In [12] is proved that antenna bending broadens the radiation pattern in the bending plane which results to a drop of gain. In [13] the authors suggest that the larger the bending of the surface the more the decrease in the maximum realized gain value of the antenna. This is proved also here when mounting the antenna to the plastic part retrieved from the A-pillar of the vehicle. This plastic has a smaller radius than the mirror cover and as a result is more curved. The efficiency and the value of the maximum realized gain of antenna B are decreased as stated in the Table 3. The radiation patterns of the antenna are more affected when the antenna is placed on the plastic part from the A-pillar of the vehicle.

Comparing the measured results of antenna B when placed on the automotive plastic parts it is understood that the antenna B has the maximum value of the realized gain at both frequency bands when it is mounted on the flat ABS of the trunk lid. The measured radiation patterns at both frequencies for this placement, agree well with the simulated results. When mounting the antenna on the curved ABS surfaces of the mirror cover and the A-pillar plastic, the value of the maximum realized gain decreases. An increase in the bending of the surface results in a decrease in the value of the maximum realized gain and deterioration of the radiation patterns. Moreover, at 5.9 GHz, the efficiency of the antenna B on the curved mirror cover and the A-pillar plastic is 31% and 22% respectively. This low efficiency values can also be a result of loss of the resonance at this frequency. At both [12] and [13] the antennas lost the resonance at some frequencies when bending them.

5 Conclusion

In this paper the effects of the shape and surface of automotive plastic parts on the efficiency, gain and radiation patterns of two flexible dual-band antennas were investigated for the first time, to the best of the author's knowledge. From the experiments and analysis of measurements, the mirror cover is a preferred location to mount the C-V2X antenna. The curvature of the mirror cover compared to the antenna size does not impede the antenna performance. The trunk lid which is a flat surface is also compatible with C-V2X antennas.

The antenna tested in this research resembles a dipole, which means that the current flows through the bowtie and the meander lines. By mounting the antenna at the inside of the mirror cover, the axis on which the current flows is not bent significantly and as a result the current flow is not impeded. The antenna performance is not severely affected.

Automotive antennas can be mounted inside side mirror covers or trunk lids without impeding their radiation patterns. As a next step, the antennas can be 3-D printed on automotive plastics using additive manufacture (AM) techniques and disperse the amount of antennas on the rooftops of the vehicles.

6 References

1 Koch, N. 'Vehicular spoiler antenna for high data rate wlan'. In: 2015 Loughborough Antennas & Propagation Conference (LAPC). (IEEE, 2015. pp. 1–4

2 Abbas, T., Karedal, J., Tufvesson, F.: 'Measurement-based analysis: The effect of complementary antennas and diversity on vehicle-to-vehicle communication', *IEEE Antennas and Wireless Propagation Letters*, 2013, **12**, pp. 309–312

3 Imai, S., Taguchi, K., Kashiwa, T., Kawamura, T. 'Effects of car body on radiation pattern of car antenna mounted on side mirror for inter-vehicle communications'. In: 2014 IEEE Antennas and Propagation Society International Symposium (APSURSI). (IEEE, 2014. pp. 601–602

4 Virothu, S., Anuradha, M.S. 'Flexible circularly polarized antenna for lte-v2x/5g vehicular safety applications'. In: 2021 International Conference on Computing, Communication, and Intelligent Systems (ICCCIS). (IEEE, 2021. pp. 814–821

5 Marantis, L., Paraskevopoulos, A., Rongas, D., Kanatas, A., Oikonomopoulos.Zachos, C., Voell, S. 'A printed monopole espar antenna for truck-to-truck communications'. In: 2017 International Workshop on Antenna Technology: Small Antennas, Innovative Structures, and Applications (iWAT). (IEEE, 2017. pp. 239–242

6 Asghar, M.E., Wollenschläger, F., Asgharzadeh, A., Singh, J., Hein, M.A. 'Influence of antenna mounting location on the radiation pattern of an automotive antenna'. In: 12th European Conference on Antennas and Propagation (EuCAP 2018). (IET, 2018. pp. 1–5

7 Singh, J., Neumann, A., Wack, T., Koppe, T., Stephan, R., Hein, M.A. 'Novel conformai automotive di-patch antenna verified through car door frame measurements'. In: Antennas and Propagation Conference 2019 (APC-2019). (IET, 2019. pp. 1–5

8 Chletsou, A., Locke, J.F., Papapolymerou, J.: 'Vehicle platform effects on performance of flexible, lightweight, and dual-band antenna for vehicular communications', *IEEE Journal of Microwaves*, 2021, **2**, (1), pp. 123–133

9 Rogers: 'Datasheet of rogers3850 dielectric', , 2003, pp. 1–4

10 Chletsou, A., He, Y., Locke, J.F., Papapolymerou, J. 'Multi-band, flexible, lightweight antenna on lcp for automotive applications'. In: 2020 IEEE International Symposium on Antennas and Propagation and North American Radio Science Meeting. (IEEE, 2020. pp. 1507–1508

11 Kellomaki, T., Heikkinen, J., Kivikoski, M. 'Effects of bending gps antennas'. In: 2006 Asia-Pacific Microwave Conference. (IEEE, 2006. pp. 1597–1600

12 Salonen, P., Keskilammi, M., Rahmat.Samii, Y. 'Textile antennas: Effect of antenna bending on radiation pattern and efficiency'. In: 2008 IEEE Antennas and Propagation Society International Symposium. (IEEE, 2008. pp. 1–4

13 Vallozzi, L., Rogier, H. 'Effects of bending on the radiation characteristics of a textile patch antenna'. In: 8th UGent PhD symposium. (, 2007.